Optical absorption and photoluminescence in the ternary chalcopyrite semiconductor $AgInSe_2$

Shunji Ozaki[a] and Sadao Adachi

Department of Electronic Engineering, Faculty of Engineering, Gunma University, Kiryu-shi, Gunma 376-8515, Japan

(Received 25 November 2005; accepted 3 October 2006; published online 12 December 2006)

Optical-absorption and photoluminescence (PL) spectra have been measured on the ternary chalcopyrite semiconductor $AgInSe_2$ at $T=13-300$ K. The direct-band-gap energy E_g of $AgInSe_2$ determined from the optical absorption measurements shows unusual temperature dependence at low temperatures. The resultant temperature coefficient $\partial E_g/\partial T$ is found to be positive at $T<125$ K and negative above 125 K. The PL spectra show asymmetric emission bands peaking at ~ 1.18 and ~ 1.20 eV at $T=13$ K, which are attributed to donor-acceptor pair recombinations between exponentially tailed donor states and acceptor levels. An energy-band scheme has been proposed for the explanation of the peculiar PL emission spectra observed in $AgInSe_2$. © *2006 American Institute of Physics*. [DOI: 10.1063/1.2400804]

I. INTRODUCTION

A family of the ternary semiconducting compounds $A^{I}B^{III}C^{VI}_2$ have been widely investigated because of their potential applications to photovoltaic solar cells, light emitting diodes, and nonlinear optical devices.[1,2] Most of these compounds have chalcopyrite structure in space group of D_{2d}^{12}.[3] Silver indium diselenide ($AgInSe_2$) is one in this family and has a nearly ideal chalcopyrite structure ($c/a=1.92$ and $u=0.25$).[4] Although the material has been the subject of many research efforts, many fundamental properties are not sufficiently evaluated or even unknown.[3]

Little is known about the optical properties of $AgInSe_2$.[4–10] Shay *et al.*[5] performed photoluminescence (PL) and electrolyte electroreflectance measurements on phosphor-doped $AgInSe_2$ crystals. The measured spectra indicated that $AgInSe_2$ is a direct-band-gap semiconductor having the lowest direct-band-gap energy of $E_g \sim 1.24$ eV. They found that E_g of this material is almost temperature independent between 77 and 300 K within the experimental accuracy (±5 meV). Rife *et al.*[6] studied fundamental reflectivity of polycrystalline $AgInSe_2$ in the 2–26 eV photon-energy range at $T=80$ K. They identified many interband-transition structures at various critical points. The photoconductivity measurements have been carried out by Aliyev *et al.*[7] on a Bridgman-grown $AgInSe_2$ crystal from 77 to 300 K, and obtained positive temperature-coefficient value of dE_g/dT below 120 K. The optical absorption measurements have also been carried out on $AgInSe_2$ at room temperature, yielding a direct-band-gap energy of 1.21–1.25 eV.[8–10]

In this paper, we present the optical absorption and PL spectra for $AgInSe_2$ measured at $T=13-300$ K. The temperature dependence of the lowest-band-gap energy E_g will be determined from the optical absorption measurements. The data of E_g on T will be analyzed by considering the effects of thermal expansion and electron-phonon interaction. No data are available on the temperature dependence of PL emission in $AgInSe_2$ to date. We will observe two PL emission bands peaking at ~ 1.18 and ~ 1.20 eV at $T=13$ K. These emission bands are attributed to transitions from the exponentially tailed donor states to acceptor levels. The exponentially tailed donor states may be caused by a large number of donors originating from the cation defects in the ternary chalcopyrite semiconductors.[11–13] An energy-band scheme will also be proposed for the explanation of the PL emissions in $AgInSe_2$.

II. EXPERIMENT

The $AgInSe_2$ crystals used in this study were grown by the conventional Bridgman method. The quartz ampoule graphitized by acetone was filled with a charge of Ag:In:Se=1:1:2 mixture in atomic ratio and then sealed off under 10^{-6} Torr. Ag, In, and Se were 99.9999% pure. The ampoule was slowly heated to 1000 °C, melted, and then equilibrated for at least 2 days. The crystals were grown by slowly lowering the ampoule to achieve its cooling rate of ~1.5 °C/h.

The $AgInSe_2$ crystals obtained were polycrystalline with grain size of several mm^3. They were not contained spurious phases, such as Ag_2Se and In_2Se_3. The x-ray diffraction trace for $AgInSe_2$ showed that the angles and relative strengths of the diffraction peaks were in good agreement with those reported by Gržeta-Plenković *et al.*[14] ($a=6.1$ Å and $c=11.7$ Å). The hot-probe measurements suggested that the electrical conductivity of the samples is n type. The samples were prepared by cutting the ingot with a wire saw, by mechanically polishing, and finally by chemically etching with a solution of Br_2 in methanol. Thickness of the samples was ~0.1 mm

The halogen lamp was used for optical absorption measurements, and the 488.0 nm line of an Ar^+-ion laser (NEC GLG3110) chopped at 320 Hz was used as the excitation light source for PL measurements. The optical absorption and PL spectra were taken in the 1.0–1.3 eV photon-energy

[a]Electronic mail: ozaki@el.gunma-u.ac.jp

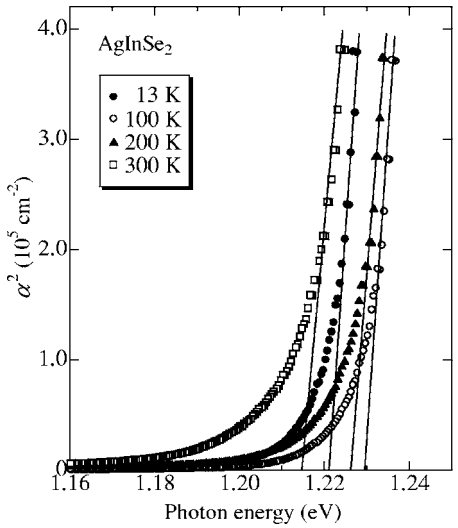

FIG. 1. Plots of the square of the absorption coefficient α^2 vs photon energy for $AgInSe_2$ at $T=13-300$ K. The intercept point on the energy axis gives the band-gap energy E_g at each temperature.

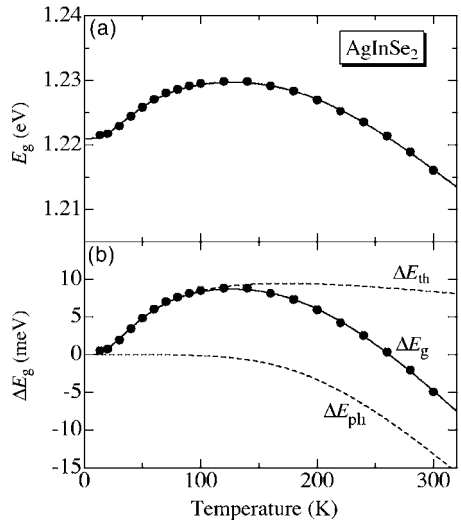

FIG. 2. (a) Plots of E_g vs T for $AgInSe_2$ determined from the optical absorption measurements. The solid line represents the least-squares fit of the experimental $E_g(T)$ data to Eq. (3). (b) Plots of ΔE_g vs T for $AgInSe_2$, together with those for ΔE_{th} and ΔE_{ph} calculated from Eqs. (4) and (9), respectively. The solid circles represent the experimental data.

range using a grating spectrometer (JASCO CT-25C) and a liquid-nitrogen cooled Ge photodiode (Hamamatsu B6175-05). The spectral resolution of the grating spectrometer used was about ±0.1 nm (±0.2 meV) at the band edge of $AgInSe_2$. The measurements were performed using a closed-cycle refrigerator cryostat (IWATANI CRT105PL) between $T=13$ and 300 K. Note that the experiments were carried out on a few grains of the polycrystalline samples. No attention was, therefore, paid to the polarization dependence of the optical spectra.

III. RESULTS AND DISCUSSION

A. Optical absorption measurements

One of the most important parameters characterizing semiconducting properties is the band-gap energy E_g. In order to determine the fundamental band-gap energy of $AgInSe_2$, we measured optical absorption spectra of the material. The absorption coefficient α was determined from the experimental transmittance T using the relation

$$T=\frac{(1-R)^2e^{-\alpha x}}{1-R^2e^{-2\alpha x}}, \tag{1}$$

where R is the reflectivity. We used a value of $R=0.23$ which was determined from our ellipsometry measurements.[15]

Figure 1 shows the experimental absorption spectra measured at $T=13-300$ K for $AgInSe_2$. The dependence of α on photon energy E can be expressed as

$$\alpha(E)=A(E-E_g)^n, \tag{2}$$

where $n=1/2$ and 2 correspond to the direct and indirect absorption gaps, respectively. We found that the fit is superior for $n=1/2$ than for 2. The fact suggests that $AgInSe_2$ is a direct-band-gap semiconductor, in agreement with those reported in the literature.[1,5,8,10]

As easily understood from Fig. 1, the optical absorption spectrum for $AgInSe_2$ exhibits unique temperature dependence. It shifts toward higher energy side with increasing temperature from 13 to 100 K. The plots in Fig. 1 give the band-gap energies of $E_g \sim 1.222$ eV at $T=13$ K and ~ 1.229 eV at $T=100$ K, respectively. Note that most of the semiconductors, such as GaAs and CdSe, exhibit only a gradual decrease of E_g from 0 to ~ 100 K (see Fig. 4). Above $T \sim 100$ K, the α^2 vs T plots for $AgInSe_2$ shifted toward lower energy side with increasing T, suggesting a decrease of E_g with increasing T. The E_g values determined in Fig. 1 at $T=200$ and 300 K are ~ 1.227 and ~ 1.216 eV, respectively.

Figure 2(a) plots the E_g vs T data for $AgInSe_2$ determined from the optical absorption measurements at $T=13-300$ K. The band-gap energy is found to increase with increasing T from 13 to $\sim 100-150$ K, and decreases with further increase of T. As mentioned before, no clear increase of E_g with increasing T has been observed in most semiconductors, such as GaAs and CdSe. Note that CdSe is the binary semiconductor analogous to $AgInSe_2$ in the sense that the average of ⟨AgIn⟩ is Cd. An increase of E_g with increasing T has also been observed in some chalcopyrite-type semiconductors, such as $AgGaS_2$, $AgGaSe_2$, $CuInS_2$, and $CuGaSe_2$.[16–20]

Recently, we performed photoreflectance (PR) measurements on $AgInSe_2$ and observed the $n=1$ exciton peaks at the $E_{0\alpha}$ (α=A, B, and C) edges.[21] It is found that the E_g vs T data shown in Fig. 2 is essentially the same as those obtained by the PR measurements. We thus consider that the observed decrease in E_g with decreasing temperature (Fig. 2) is not due to the dominance of the bound over the free excitons at low temperatures as reported in Ref. 20.

Traditionally, temperature variation of the band-gap energy $E_g(T)$ is expressed in terms of Varshni's formula.[22] Recently, Pässler[23,24] proposed an analytical expression which takes into account the band-gap shrinkage effect in accordance with general equations and parameter relationships governing the electron-phonon interaction mechanism. Pässler's expression is more palatable than Varshni's equa-

tion from the theoretical point of view. However, we found that these two expressions cannot completely describe the temperature dependence of E_g observed for $AgInSe_2$.

It is well known that the temperature shift of E_g is arising from the effects of not only electron-phonon interaction (ΔE_{ph}) but also thermal expansion (ΔE_{th}),[25]

$$E_g(T) = E_g(0) + \Delta E_g(T) = E_g(0) + \Delta E_{ph}(T) + \Delta E_{th}(T). \tag{3}$$

Practically, it is very difficult to separate these two components experimentally. However, it is possible to calculate the linear thermal expansion effect if the interband hydrostatic deformation potential a_H and the linear thermal expansion coefficient α_{th} are known,[26–28]

$$\Delta E_{th}(T) = 3a_H \int_0^T \alpha_{th}(T')dT'. \tag{4}$$

In calculating Eq. (4), we require the values of a_H and $\alpha_{th}(T)$ for $AgInSe_2$. However, no experimental a_H data are available and only the limited α_{th} values ($T \geqslant 80$ K) have been experimentally determined to date. Wei *et al.*[29] presented the results of a first-principles calculation of the direct-band-gap pressure coefficient a_H for a series of Ga-based and In-based chalcopyrite semiconductors, including $AgInSe_2$ (a_H=1.03 eV). An exact calculation of $\alpha_{th}(T)$ [$\Delta E_{th}(T)$] is also possible theoretically, but the lack of knowledge of various parameters and the difficulty of obtaining exact solution of phonon-phonon interactions are usually formidable barriers to progress. In the following, we obtain $\Delta E_{th}(T)$ based on the simple expressions of the solid-state physics.

The linear thermal expansion coefficient α_{th} is proportional to the specific heat C_v at constant volume (Ref. 30),

$$\alpha_{th} = \frac{1}{3}\frac{\gamma C_v C_0}{V} = \frac{1}{9}\frac{\gamma C_v}{V B_u}, \tag{5}$$

where γ is the averaged Grüneisen parameter, C_0 is the isothermal compressibility, B_u is the bulk modulus, and V is the volume of the crystal. α_{th} is known to depend markedly on T and is positive at high temperatures for most semiconductors.[31–33]

The Debye model for lattice vibrational energy yields in the relation[30]

$$C_p \sim C_v = 3RF(\theta_D/T), \tag{6}$$

where θ_D is the Debye temperature and $F(\theta_D/T)$ is the Debye function defined by

$$F(\theta_D/T) = (T/\theta_D)^3 \int_0^{\theta_D/T} \frac{3x^4 e^x}{(e^x - 1)^2} dx, \tag{7}$$

R is the gas constant. In the low-temperature limit ($T \ll \theta_D$), $F(\theta_D/T)$ is approximated to be $(4/5)\pi^4(T/\theta_D)^3$, then $C_v \sim (12/5)\pi^4 R(T/\theta_D)^3$ (Debye's T^3 law). In the high-temperature limit ($T \gg \theta_D$), on the other hand, $F(\theta_D/T)$ becomes to be unity, then $C_v \sim 3R$ (Dulong-Petit's law).

In Fig. 3, we show the temperature variations of (a) C_v, (b) γ, and (c) α_{th} for $AgInSe_2$. The C_v vs T data are calculated from Eq. (6) using a value of θ_D=191 K.[34] The $\alpha_{th}(T)$ plots are obtained by calculating a semiempirical quasiharmonic fit,[30]

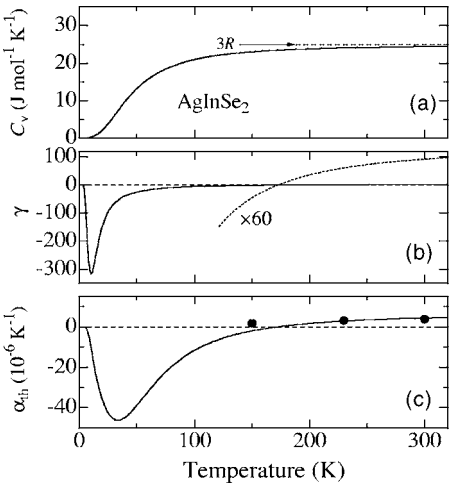

FIG. 3. Temperature variations of (a) C_v, (b) γ, and (c) α_{th} for $AgInSe_2$. $C_v(T)$ are calculated from Eq. (6) using a value of θ_D=191 K, while $\alpha_{th}(T)$ are obtained by calculating a semiempirical quasiharmonic fit expression of Eq. (8). $\gamma(T)$ in (b) are finally obtained by inserting $C_v(T)$ [(a)] and $\alpha_{th}(T)$ [(c)] into Eq. (5). The horizontal arrow in (a) corresponds to a value of C_v in the high-temperature limit $T \to \infty$ ($C_v \sim 3R$, Dulong-Petit's law). The solid circles in (c) represent the experimental data of $\alpha_{th}=(\alpha_{\parallel}+2\alpha_{\perp})/3$ measured by Orlova and Bodnar (Ref. 35).

$$\alpha_{th}(T) = \sum_{i=1}^{3} X_i \frac{(\theta_i/T)^2 \exp(\theta_i/T)}{[\exp(\theta_i/T) - 1]^2}, \tag{8}$$

with $X_1 = -6.0 \times 10^{-5}$ K^{-1}, θ_1=50 K, $X_2 = 7.7 \times 10^{-5}$ K^{-1}, θ_2=230 K, $X_3 = -1.0 \times 10^{-5}$ K^{-1}, and θ_3=400 K. The solid circles in Fig. 3(c) correspond to the experimental $\alpha_{th}=(\alpha_{\parallel}+2\alpha_{\perp})/3$ data measured by Orlova and Bodnar,[35] where $\alpha_{\parallel}$ and $\alpha_{\perp}$ represent the thermal expansion values along and perpendicular to the c axis, respectively. Note that our estimated α_{th} value shows a sign reversal at $T \sim 170$ K. It is known that Si, Ge, and most III-V and II-VI semiconductors also show a sign reversal in the thermal expansion coefficient below about 100 K.[31–33] On the other hand, diamond and 3C-SiC exhibit no negative thermal expansion even at low temperatures.[31] Biernacki and Scheffler[36] suggested from density-functional-theory calculations of thermodynamic potentials that the origin of the negative expansion coefficient is traced back to the entropy contribution of the Gibbs free energy.

Usually γ is calculated from Eq. (5), where α_{th}, C_v, C_0 (B_u), and V are experimentally measured quantities. The $\gamma(T)$ values plotted in Fig. 3(b) were calculated by inserting $C_v(T)$ [Fig. 3(a)] and $\alpha_{th}(T)$ [Fig. 3(c)] into Eq. (5). The $B_u = 1/(3C_0)$=58.5 GPa value was taken from Ref. 29. The Grüneisen parameter γ can describe the deviation of the phonon spectrum from the harmonic approximation. At $T \geqslant \theta_D$, γ is known to be a constant, whose value depends on the nature of the forces present in the crystal and usually ranges from 1 to 3. Our obtained γ value in Fig. 3(b) is about 1.5 at $T \sim 300$ K. The parameter γ serves as a measure of the anharmonicity of the vibrations of the atoms in the crystals. From Fig. 3(b), we expect a very stronger anharmonic lattice

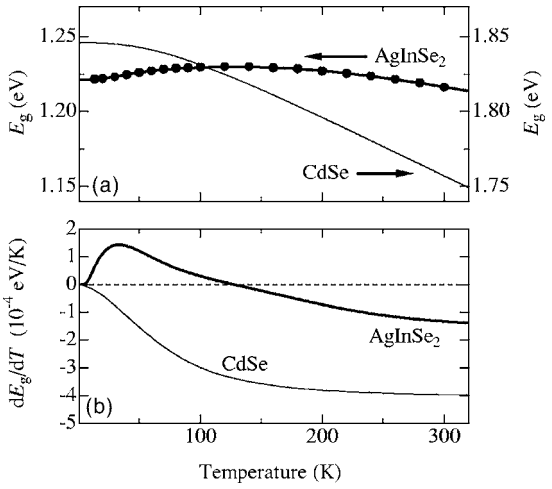

FIG. 4. Plots of (a) E_g vs T and (b) dE_g/dT vs T for $AgInSe_2$ and CdSe. The experimental data for CdSe are taken from Ref. 33.

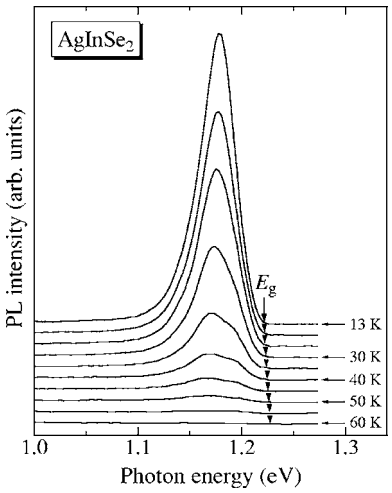

FIG. 5. PL spectra of $AgInSe_2$ measured at $T=13-60$ K. The vertical arrows indicate the positions of the bandgap energy E_g.

potential of $AgInSe_2$ at lower temperatures. Similarly, CuCl, which is one of the most ionic semiconductors crystallizing in the zinc-blende structure, exhibits a number of peculiarities that have been associated with a strongly anharmonic lattice potential, e.g., a strongly negative thermal expansion coefficient at low temperatures and elastic shear constants that decrease with increasing hydrostatic pressure, together with a large positive temperature variation of the bandgap energy dE_g/dT up to $T=350$ K.[37]

The electron-phonon interaction term ΔE_{ph} in Eq. (3) can be given by the same form as proposed by Pässler,[23,24]

$$\Delta E_{\mathrm{ph}}(T) = \frac{\alpha_p \Theta_p}{2}\left[\sqrt[p]{1+\left(\frac{2T}{\Theta_p}\right)^p}-1\right], \tag{9}$$

where α_p plays the role of a $T\rightarrow\infty$ limiting value of the band-gap shrinkage coefficient $-\partial E_g(T)/\partial T$, Θ_p is approximately equal to the average phonon temperature, and the power exponent p is closely related to the overall shape of the electron-phonon spectral function in the given material.

The solid line in Fig. 2(a) shows the least-squares fit of the experimental E_g values to Eq. (3). The corresponding ΔE_{th} and ΔE_{ph} values as calculated from Eqs. (4) and (9), respectively, are shown in Fig. 2(b). The value of $a_H=-1.03$ eV used in Eq. (4) was taken from Ref. 29. The values of $\alpha_p=0.14$ meV/K, $\Theta_p=430$ K, and $p=4.9$ were also used in Eq. (9). It is recognized from Fig. 2(a) that Eq. (3) provides an excellent agreement with the experimental data over the entire temperature range ($T=13-300$ K). It is also seen that an increase of E_g at $T=13-100$ K can be successfully explained by the negative lattice thermal expansion of $AgInSe_2$.

It is noted that E_g of $AgInSe_2$ is about 0.6 eV smaller than that of the binary analogous semiconductor CdSe (see Fig. 4 and Ref. 33). This may be due to the hybridization of the d orbitals of cation (Ag) with the p orbitals of anion (Se).[1,38] When the chalcopyrite lattice suffers dilatation, the cation-anion distance increases, the p-d admixture reduces, and as a result, the band-gap energy increases. Therefore, the temperature coefficient dE_g/dT of $AgInSe_2$ is positive in the negative thermal expansion region ($T=0-125$ K), as plotted in Fig. 4(b). For $T>125$ K, the electron-phonon contribution becomes dominant, then the coefficient dE_g/dT becomes negative and its absolute value gradually increases with increasing T. Further increase of T gives a saturated value of $dE_g/dT=-1.4\times10^{-4}$ eV/K. Similarly, Aliyev *et al.*[7] measured photoconductivity spectra of $AgInSe_2$ from $T=77$ to 300 K and obtained positive dE_g/dT value of $\sim+5\times10^{-4}$ eV/K below 120 K and negative value of $\sim-1.5\times10^{-4}$ eV/K at $T=120-300$ K. The positive value was explained by the lattice dilatation effect being the dominant mechanism for the band-gap shift at $T\leqslant120$ K.

In the case of the binary analogous semiconductor CdSe (Ref. 32), the temperature coefficient dE_g/dT in the limit $T\rightarrow0$ K is ±0, gradually decreases with increasing T, and finally shows a saturated value of $dE_g/d_T=-4\times10^{-4}$ eV/K at high temperatures [Fig. 4(b)]. The thermal expansion data reported for CdSe are in the range $T=300-900$ K.[33] These data show positive α_{th} values. Judging from another II-VI and III-V data in Refs. 32 and 33, however, we expect that CdSe has negative thermal expansion coefficients at temperatures below roughly about 100 K. It should be noted, however, that the thermal expansion term ΔE_{th} in such tetrahedrally coordinated semiconductors is much smaller than the electron-phonon term ΔE_{ph}. In fact, it is found that the thermal expansion contribution ΔE_{th} accounts for only 7% of the total temperature shift ΔE_g at $T=300$ K for ZnO (Ref. 39) and for 16% (4%) at $T=300$ K (100 K) for GaP.[28] Thus, no positive temperature variation of the band-gap energy has been observed in ZnO, GaP, or CdSe semiconductors even at low temperatures. No positive variation of dE_g/dT has also been observed in all II-VI or III-V semiconductors, except for HgSe and HgTe which are known as the semimetallic materials and have a value of $dE_g/dT\sim+7\times10^{-4}$ eV/K.[30,31]

B. PL measurements

Figure 5 shows the PL spectra for $AgInSe_2$ obtained at temperatures between $T=13$ and 60 K. The vertical arrow indicates the position of the band-gap energy E_g at each temperature determined by the optical absorption measurements.

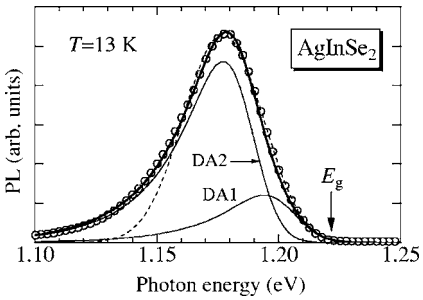

FIG. 6. Theoretical fit of the PL spectrum for $AgInSe_2$ measured at $T=13$ K. The dashed line represents the DA-pair emissions obtained from Eq. (10), while the heavy solid line shows those from Eq. (13). The light solid lines represent the deconvolution of the heavy solid line into two individual peaks (DA1 and DA2). The vertical arrow indicates the position of the bandgap energy at $T=13$ K.

No clear PL emission has been observed at $T>60$ K. It is evident from Fig. 5 that the PL spectrum at $T\leqslant 40$ K shows the dominant peak at ~1.18 eV (DA2). As the temperature increases from 13 K, the ~1.18 eV emission intensity becomes weak and, as a result, the high-energy shoulder can be clearly observed at an energy of ~1.20 eV (DA1) for $T\geqslant 30$ K. No clear band-edge emission has been observed over the temperature range investigated ($T=13-300$ K).

The donor-acceptor (DA) pair emission band can be modeled using a Gaussian line shape as

$$I_{\mathrm{DA}}(E)=S_{\mathrm{DA}}\exp\left[-\frac{(E-E_p)^2}{\Gamma^2}\right], \tag{10}$$

where E_p is the DA-pair emission peak energy, and S_{DA} and Γ are the strength and spectral width parameters, respectively.

We show in Fig. 6 the fitted result of the experimental PL spectrum measured at $T=13$ K (open circles) to Eq. (10) by taking into account the two Gaussian peaks, DA1 and DA2 (dashed line). It is evident from Fig. 6 that the simple Gaussian line-shape model gives no good agreement with the experimental data, especially at photon energies below 1.16 eV.

In order to achieve the better fit with the experimental data, we assume that the density of states in the conduction-band tail of the DA1 and DA2 bands depends exponentially on the energy distance from the unperturbed conduction-band edge,[40]

$$N_{\mathrm{D}}(E,T)=\begin{cases}\dfrac{{N_{\mathrm{D}}}^0}{1+Ae^{-{E_{\mathrm{D}}}^{\mathrm{eff}}/kT}}\exp[m(E-E_d)], & E\leqslant E_d\\ 0, & E>E_d,\end{cases} \tag{11}$$

where ${E_{\mathrm{D}}}^{\mathrm{eff}}$ is the effective (or "center-of-gravity") energy of the exponentially tailed donor states, E_d is the so-called "demarcation level" of the donor states, ${N_{\mathrm{D}}}^0$ is the density of donor states at $E=E_d$ and $T=0$ K, and m is the slope of the conduction-band tail. Here, the ${E_{\mathrm{D}}}^{\mathrm{eff}}$ term is introduced in order to take into account the thermal excitation of the exponential donor electrons into the conduction band. The slope parameter m is assumed to be independent of T.

The exponentially tailed donor states may arise from the failure in the periodic distribution of the stoichiometric cations and anions in the chalcopyrite structure. Anedda *et al.*[41] measured the photoconductivity in defect-chalcopyrite semiconductor $CdIn_2S_4$ and found a high density ($\sim 10^{20}$ cm^{-3}) of electron trap levels with an exponential distribution in energy. They explained such higher density electron traps in terms of higher disorder in the cation sublattice. Siebentritt and Schuler[13] observed asymmetric DA-pair emission in Cu-poor $CuGaSe_2$ chalcopyrite. These authors also found a high density of the electron traps originating from the cation defects. The same electron traps as in $CdIn_2S_4$ and $CuGaSe_2$ have been observed in various isostructural ($A^{\mathrm{II}}B^{\mathrm{III}}{}_2C^{\mathrm{VI}}{}_4$ and $A^{\mathrm{I}}B^{\mathrm{III}}C^{\mathrm{VI}}{}_2$) chalcopyrite semiconductors.[1,11,12,42]

The acceptor states are assumed to exhibit a broadened Gaussian distribution given by

$$N_{\mathrm{A}}(E,T)=\frac{{N_{\mathrm{A}}}^0}{1+Be^{-E_{\mathrm{A}}/kT}}\exp\left[-\frac{(E-E_{\mathrm{A}})^2}{\Gamma^2}\right], \tag{12}$$

where ${N_{\mathrm{A}}}^0$ is the acceptor concentration, E_{A} is the acceptor ionization energy, and Γ is the width parameter of the acceptor states.

The resultant DA-pair recombination intensity $I_{\mathrm{DA}}(E,T)$ can be given by the convolution integral as[40]

$$I_{\mathrm{DA}}(E,T)=P_{\mathrm{DA}}\int N_A(E',T)N_D(E'+E,T)dE', \tag{13}$$

where P_{DA} is the DA-pair transition probability which is assumed to be independent of E and T. The parameters Γ and E_d influence essentially the peak width and asymmetry of the spectrum, respectively. The m value to be fit determined below is 47 eV^{-1}.

The heavy solid line in Fig. 6 shows the fitted result of the experimental PL spectrum using Eq. (13) for the DA1 and DA2 emissions. Individual contributions of the DA1 and DA2 emission bands are shown in Fig. 6 by the light solid lines. Assuming the exponentially tailed donor density of Eq. (11), the theoretical calculation begins to give good agreement with the experimental spectrum over the entire photon-energy range. Note that this type of luminescence has been commonly found in spectra of the $A^{\mathrm{I}}B^{\mathrm{III}}C^{\mathrm{VI}}{}_2$ [$AgInTe_2$,[43] $AgGaS_2$,[44] $AgGaSe_2$,[44] $CuInSe_2$,[45] and $A^{\mathrm{II}}B^{\mathrm{III}2}C^{\mathrm{VI}}$ chalcopyrite semiconductors [$CdGa_2Se_4$,[46] $CdGa_2Te_4$,[47] $CdIn_2Te_4$,[48] $ZnGa_2Se_4$,[49] $ZnIn_2Te_4$ (Ref. 50)]. Dirnstorfer *et al.*[51] also observed asymmetric DA-pair emission from In-rich $CuIn(Ga)Se_2$ films and explained its temperature and excitation intensity dependences using the Shklovskij/Efros model.

Let us show in Fig. 7(a) the temperature dependence of the DA-pair emission energies, E_p (DA1) and E_p (DA2), and the demarcation level width E_d for $AgInSe_2$. For comparison, the temperature dependence of E_g is plotted by the heavy solid line. As seen in the Fig. 7(a), $E_g(T)$ gradually increases with increasing T from 13 to 60 K, while E_p and E_d decrease with increasing T. The temperature coefficients for E_p (DA1) and E_p (DA2) are determined to be about -2×10^{-4} and -4×10^{-4} eV/K, respectively.

The DA-pair emission energy is theoretically expressed as $E_p(T)=E_g(T)-E_{\mathrm{A}}-E_{\mathrm{D}}+(e^2/4\pi\varepsilon r)$, where r is the paired

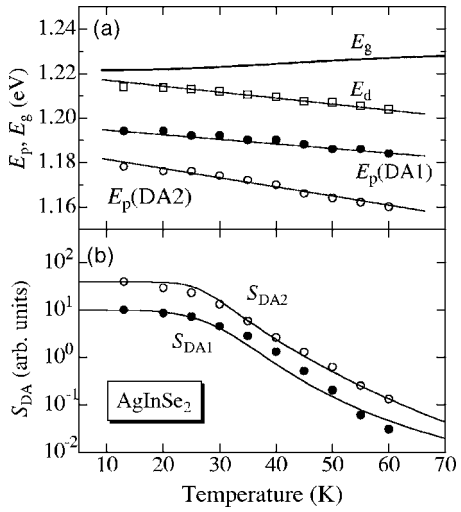

FIG. 7. (a) Variations of the band-gap energy E_g, "demarcation level" width E_d, and DA-pair peak energies E_p's as a function of temperature T for $AgInSe_2$. (b) Variations of the strength parameters S_{DA1} and S_{DA2} as a function of temperature T for $AgInSe_2$. The solid lines show the calculated results of Eq. (14).

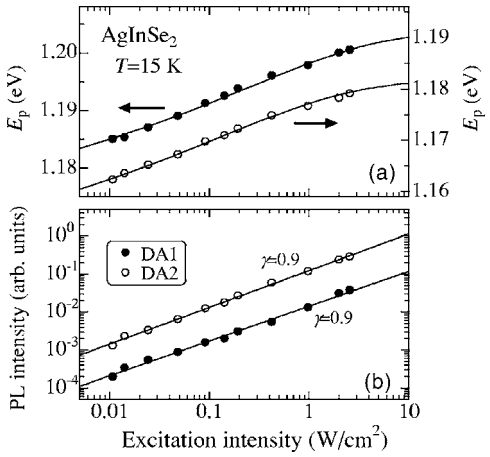

FIG. 8. (a) Excitation intensity dependence of the PL peak energies E_p's and (b) integrated PL intensities for the DA1 and DA2 emissions in $AgInSe_2$ at T=15 K. The solid lines in (a) and (b) are calculated from Eqs. (16) and (17), respectively.

DA distance. The lowest possible DA-pair energy is given in the limit $r \rightarrow \infty$ by $E_p(T)=E_g(T)-E_A-E_D$. The dependence of E_p on T may, thus, be very similar to $E_g(T)$. This is, however, not the case for E_p (DA1) and E_p (DA2).

In the case of the exponential-donor-acceptor-pair emission, we suppose that the DA-pair separation r increases as T increases due to the thermal ionization of carriers bound to acceptors and donors.[52] As a result, the DA-pair emission peak should shift to lower energies with increasing T due to the decrease of the Coulomb term $e^2/4\pi\varepsilon r$. This should explain the variations of E_p and E_d with T observed in Fig. 7(a), as has also been found in $CuGa_3Se_5$.[52]

The temperature-dependent strength parameter of the DA-pair emission can be written from Eqs. (11)–(13) as

$$S_{DA}(T)=\frac{S_{DA}{}^0}{(1+Ae^{-E_D{}^{eff}/kT})(1+Be^{-E_A/kT})}, \tag{14}$$

with

$$S_{DA}{}^0=N_D{}^0N_A{}^0P_{DA}, \tag{15}$$

where P_{DA} is the transition strength parameter of the DA-pair emission.

Figure 7(b) shows the variations of S_{DA1} and S_{DA2} as a function of temperature T. The solid lines represent the calculated results of Eq. (14) with $S_{DA1}{}^0=10$, $A=3.0\times10^3$, and $B=35$ (DA1); $S_{DA2}{}^0=39$, $A=1.1\times10^4$, and $B=240$ (DA2), respectively. The activation energies determined here are $E_A=10$ meV (DA1) and 27 meV (DA2). The $E_D{}^{eff}$ value is also determined to be 23 meV (DA1 and DA2).

The PL spectra observed in $AgInSe_2$ showed the two asymmetric DA-pair emission bands, DA1 and DA2. In order to confirm these two bands as actually due to the DA-pair emissions, we examined the excitation intensity dependence of the PL peak energy and integrated emission intensity at T=15 K. Figure 8 indicates the results of these experiments. It is evident from Fig. 8(a) that the DA1 (DA2) peak energy E_p increases from 1.185 (1.162) to 1.201 eV (1.179 eV) as the laser excitation intensity increases from 0.01 to 3 W/cm^2. For the DA-pair recombination, the excitation laser power I_{ex} can be expressed, as a function of PL peak energy E_p, as[53]

$$I_{ex}=I_0\frac{(E_p-E_\infty)^3}{(E_B-E_\infty-2E_p)}\exp\left(-\frac{2(E_B-E_\infty)}{E_p-E_\infty}\right), \tag{16}$$

where I_0 is a proportionality constant, E_B is the emitted photon energy of a close DA pair separated by a shallow-impurity Bohr radius, and E_∞ is the emitted photon energy of an infinity distant DA pair. The solid lines in Fig. 8(a) represent the fitted results of the experimental E_p values to Eq. (16). The fit-determined DA1 (DA2) parameters are E_B =1.25 eV (1.23 eV) and E_∞=1.16 eV (1.13 eV). We can see that these parameters satisfy the DA-pair emission requirement of $E_\infty \leqslant E_p$=1.185–1.201 eV (E_p=1.162–1.179 eV) $\leqslant E_B$ for the DA1 (DA2) emission.

The integrated PL intensity I vs I_{ex} can be given by the simple power law,[53]

$$I \propto I_{ex}{}^\gamma. \tag{17}$$

The dimensionless exponent γ is known to be $1<\gamma<2$ for free-exciton or bound-exciton emission and $\gamma \leqslant 1$ for free-to-bound or DA-pair emission. The solid lines in Fig. 8(b) represent the fitted results of the experimental data to Eq. (17). The γ value, 0.9, supports the assignment of these PL emissions to DA-pair recombination at least for T=15 K. The relatively strong thermal quenching of the PL intensity is a formidable barrier to make the same assignment at high temperatures.

We finally show in Fig. 9 the schematic energy-band diagram and PL transitions observed in $AgInSe_2$ for T =13 K. The conduction-band and valence-band densities of states can be represented by the well-known expressions of $N_C \propto (E-E_C)^{1/2}$ and $N_V \propto (E_V-E)^{1/2}$, respectively. The exponentially tailed donor states of Eq. (11) and broadened Gaussian-like acceptor states of Eq. (12) are also plotted in Fig. 9. The acceptor ionization energies determined from the

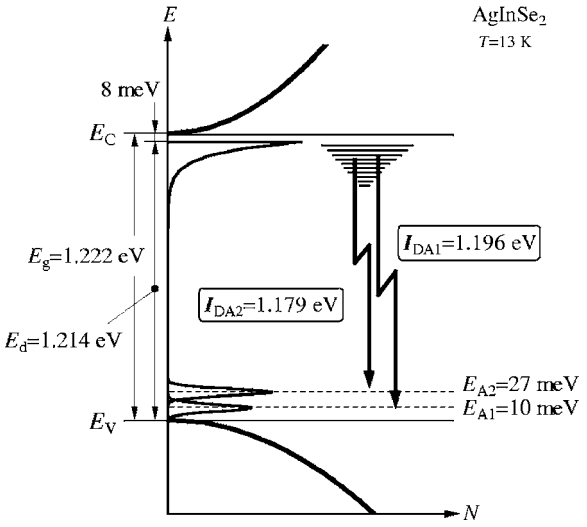

FIG. 9. Proposed energy-band scheme and optical transitions in $AgInSe_2$ at $T=13$ K.

temperature-dependent PL intensities are centered at 10 and 27 meV above the top of the valence band for DA1 and DA2, respectively.

The PL emission caused by transitions from the exponentially tailed donor state to acceptor levels showed the typical DA-pair recombination characteristics, as demonstrated in Fig. 8. The photogenerated electrons in the conduction band can be efficiently transferred, via energy relaxation, to the exponential-donor states. The exponential-donor-related emission is, thus, the dominant PL mechanism in $AgInSe_2$. Reflecting the exponentially tailed donor states, the DA-pair emission band observed is strongly asymmetric with tail at the low photon-energy side. The band-to-band emission has never been observed in $AgInSe_2$. This is because always $E_d < E_g$ in $AgInSe_2$ [see Fig. 7(a)]. In $ZnIn_2Te_4$, $E_d \leqslant E_g$ for $T \leqslant 90$ K and $E_d > E_g$ for $T > 90$ K, then, the band-to-band emission was observed only for $T = 90$ K.[50]

IV. CONCLUSIONS

We have measured the optical absorption and PL emission spectra on the chalcopyrite semiconductor $AgInSe_2$ at $T=13-300$ K. The direct-band-gap energy E_g of $AgInSe_2$ determined from the optical absorption spectra has shown unusual temperature dependence. The E_g value gradually increases from ~1.222 eV at $T=13$ K, exhibiting a maximum ~1.230 eV at ~130 K, and then decreases with further increase of T. The room-temperature E_g value is determined to be ~1.216 eV. The corresponding temperature coefficient dE_g/dT has positive values for $T<125$ K and negative ones above 125 K. The 300 K dE_g/dT value is -1.4×10^{-4} eV/K which is considerably smaller than those reported for many II-VI and III-V semiconductors ($\sim -4 \times 10^{-4}$ eV/K). The positive temperature coefficient of dE_g/dT in $AgInSe_2$ has been successfully explained by considering the negative lattice thermal expansion in this material. The PL spectra of $AgInSe_2$ have been shown to originate from transitions between the exponentially tailed donor state and acceptor levels. The "demarcation level" width of $E_d = 1.214$ eV and acceptor levels at 10 and 27 meV above the top of the valence band have been determined from an analysis of the low-temperature PL spectra.

[1] J. L. Shay and J. H. Wernick, *Ternary Chalcopyrite Semiconductors: Growth, Electronic Properties, and Applications* (Pergamon, Oxford, 1975).
[2] S. Chichibu, S. Shirakata, S. Isomura, and H. Nakanishi, Jpn. J. Appl. Phys., Part 1 **36**, 1703 (1997).
[3] O. Madelung, *Semiconductors: Data Handbook* (Springer, Berlin, 2004), p. 320.
[4] K. Yoshino, N. Mitani, M. Sugiyama, S. Chichibu, H. Komaki, and T. Ikari, Physica B **302–303**, 349 (2001).
[5] J. L. Shay, B. Tell, H. M. Kasper, and L. M. Schiavone, Phys. Rev. B **7**, 4485 (1973).
[6] J. C. Rife, R. N. Dexter, P. M. Bridenbaugh, and B. W. Veal, Phys. Rev. B **16**, 4491 (1977).
[7] V. A. Aliyev, G. D. Guseinov, F. I. Mamedov, and L. M. Chapanova, Solid State Commun. **59**, 745 (1986).
[8] A. El-Korashy, M. A. Abdel-Rahim, and H. El-Zahed, Thin Solid Films **338**, 207 (1999).
[9] A. H. Ammar, A. M. Farid, and M. A. M. Seyam, Vacuum **66**, 27 (2002).
[10] M. C. S. Kumar and B. Pradeep, Vacuum **72**, 369 (2004).
[11] A. N. Georgobiani, S. I. Radautsan, and I. M. Tiginyanu, Fiz. Tekh. Poluprovodn. (S.-Peterburg) **19**, 193 (1985) [Sov. Phys. Semicond. **19**, 121 (1985)].
[12] M. Guzzi and E. Grilli, Mater. Chem. Phys. **11**, 295 (1984).
[13] S. Siebentritt and S. Schuler, J. Phys. Chem. Solids **64**, 1621 (2003).
[14] B. Gržeta-Plenković, S. Popović, B. Čelustka, and B. Šantić, J. Appl. Crystallogr. **13**, 311 (1980).
[15] S. Ozaki and S. Adachi, Phys. Status Solidi A **203**, 2919 (2006).
[16] P. W. Yu, W. J. Anderson, and Y. S. Park, Solid State Commun. **13**, 1883 (1973).
[17] N. Yamamoto, H. Horinaka, and T. Miyauchi, Jpn. J. Appl. Phys. **18**, 255 (1979).
[18] J. J. M. Binsma, L. J. Giling, and J. Bloem, J. Lumin. **27**, 55 (1982).
[19] C. Bellabarba and C. Rincon, Jpn. J. Appl. Phys., Suppl. **32**, 599 (1993).
[20] A. Bauknecht, S. Siebentritt, J. Albert, Y. Tomm, and M. C. Lux-steiner, Jpn. J. Appl. Phys., Suppl. **39**, 322 (2000).
[21] S. Ozaki and S. Adachi, J. Mater. Sci.: Mater. Electron. (to be published).
[22] Y. P. Varshni, Physica (Amsterdam) **34**, 149 (1967).
[23] R. Pässler, Phys. Status Solidi B **200**, 155 (1997).
[24] R. Pässler, Phys. Status Solidi B **216**, 975 (1999).
[25] M. Cardona, Solid State Commun. **133**, 3 (2005).
[26] P. Lautenschlager, P. B. Allen, and M. Cardona, Phys. Rev. B **31**, 2163 (1985).
[27] L. Malikova, W. Krystek, F. H. Pollak, N. Dai, A. Cavus, and M. C. Tamargo, Phys. Rev. B **54**, 1819 (1996).
[28] T. Mishima, M. Miura, S. Ozaki, and S. Adachi, J. Appl. Phys. **91**, 4904 (2002).
[29] S.-H. Wei, A. Zunger, I.-H. Choi, and P. Y. Yu, Phys. Rev. B **58**, R1710 (1998).
[30] S. Adachi, *Properties of Group-IV, III-V and II-VI Semiconductors* (Wiley, Chichester, 2005).
[31] S. Adachi, *Handbook on Physical Properties of Semiconductors Volume 1: Group-IV Semiconductors* (Kluwer Academic, Boston, 2004).
[32] S. Adachi, *Handbook on Physical Properties of Semiconductors Volume 2: III-V Compound Semiconductors* (Kluwer Academic, Boston, 2004).
[33] S. Adachi, *Handbook on Physical Properties of Semiconductors Volume 3: II-VI Compound Semiconductors* (Kluwer Academic, Boston, 2004).
[34] J. B. Cáceres and C. Rincón, Phys. Status Solidi B **234**, 541 (2002).
[35] N. S. Orlova and I. V. Bodnar, Phys. Status Solidi A **101**, 421 (1987).
[36] S. Biernacki and M. Scheffler, Phys. Rev. Lett. **63**, 290 (1989).
[37] A. Göbel *et al.*, Phys. Rev. B **57**, 15183 (1998).
[38] J. L. Shay, B. Tell, H. M. Kasper, and L. M. Schiavone, Phys. Rev. B **5**, 5003 (1972).
[39] S. Ozaki, T. Mishima, and S. Adachi, Jpn. J. Appl. Phys., Part 1 **42**, 5465 (2003).
[40] E. Grilli, M. Guzzi, E. Camerlenghi, and F. Pio, Phys. Status Solidi A **90**, 691 (1985).
[41] A. Anedda, L. Garbato, F. Raga, and A. Serpi, Phys. Status Solidi A **50**, 643 (1978).
[42] P. Manca, F. Raga, and A. Spiga, Nuovo Cimento Soc. Ital. Fis., B **19B**,

15 (1974).
[43]A. Jagomägi, J. Krustok, J. Raudoja, M. Grossberg, I. Oja, M. Krunks, and M. Danilson, Thin Solid Films **480–481**, 246 (2005).
[44]B. Tell and H. M. Kasper, Phys. Rev. B **4**, 4455 (1971).
[45]H. Matsushita and T. Takizawa, Jpn. J. Appl. Phys., Part 1 **37**, 4258 (1998).
[46]G. B. Abdullaev, V. G. Agaev, V. B. Antonov, R. Kh. Nai, and É. Yu. Salaev, Fiz. Tekh. Poluprovodn. (S.-Peterburg) **6**, 1729 (1972) [Sov. Phys. Semicond. **6**, 1492 (1973)].
[47]S. Ozaki, K. Muto, H. Nagata, and S. Adachi, J. Appl. Phys. **97**, 043507 (2005).
[48]G. Couturier, B. Jean, and J. Salardenne, J. Appl. Phys. **78**, 5654 (1995).
[49]S. I. Radautsan, I. M. Tiginyanu, V. N. Fulga, and Yu. O. Derid, Phys. Status Solidi A **114**, 259 (1989).
[50]S. Ozaki, S. Boku, and S. Adachi, Phys. Rev. B **68**, 235201 (2003).
[51]I. Dirnstorfer, Mt. Wagner, D. M. Hofmann, M. D. Lampert, F. Karg, and B. K. Meyer, Phys. Status Solidi A **168**, 163 (1998).
[52]C. Rincón, S. M. Wasim, G. Marín, E. Hernández, G. S. Perez, and J. Galibert, J. Appl. Phys. **87**, 2293 (2000).
[53]N. M. Gasanly, A. Serpengüzel, A. Aydinli, O. Gürlü, and I. Yilmaz, J. Appl. Phys. **85**, 3198 (1999).